Carbon – Science and Technology

RESEARCH ARTICLE

Preparation of mesoporous carbon from fructose using zinc-based activators

Tutik Setianingsih[(A)], Indriana Kartini[(B)], Yateman Arryanto[(B)]

(A)   Department of Chemistry, Brawijaya University , Jl.Veteran 169 Malang, Indonesia .
(B)   Department of Chemistry, Gadjah Mada University, Jl. Bulaksumur Yogyakarta, Indonesia.

Mesoporous carbons were synthesized from fructose using activators of zinc silicate (ZS), zinc borate (ZB), and zinc borosilicate (ZBS). The synthesis involves 3 steps, including caramelization of sugar, carbonization of caramel, and washing of carbon to separate the activator from the carbon. The solid products were characterized by N_2 gas adsorption-desorption, X-ray diffraction, FTIR spectrophotometry, and Transmission Electron Microscopy. The pore characterizations of the carbons indicate that in ZBS system, ZB may have the role as mesopore size controller, whereas silica component may improve porosity created by ZB without changing the size. This role of ZB may be connected to it's performance as catalyst of caramelization and it's crystalinity, as supported by measurement of caramel intermediete and characterization of the activators with X-ray diffraction. The infrared spectra confirms that the carbons's surfaces have C=O, C-O, and O-H functional groups. The XRD patterns of the carbons show that all activators create the turbotratic carbons.

---

1. Introduction :

Mesoporous carbon is a porous material which has pore size of 2 – 50 nm and potential as an adsorben of large molecule [1], double layer capacitor [2], and template of other mesoporous oxides [3]. This material is usually prepared using pore template to create large pore size. Pore template could be single templates such as mesoporous silica [4], nanoparticle silica [5], or surfactant [6]. Those single templates has created mesoporous carbos with pore size distributions centered around 3 – 6.5 nm. Such small pores make those carbon can not handle adsorption of large substances (> 100 Å), for example marine bacteries with size of 300 Å [7]. Therefore, the need to create large mesopore carbon is prominent.

Some researchers reported the synthesis of mesoporous carbons with combination of more than one   template involving boric acid as

component, such as boric acid and SBA-15 silica [8] or of boric acid, TEOS, and surfactant [9, 10], colloidal silica – boric acid [11], and boric acid - nanoparticle silica [12, 13]. Those methods successfully created mesopore uniformity larger than 10 nm, but the synthesis protocols involved high carbonization temperature, i.e. 900°C.

Some researchers reported low temperature of carbonization (450 – 600°C) using $ZnCl_2$ [14 - 17]. $ZnCl_2$ can form ZBS activator system with boric acid and silica. This ceramics have a way to prepare mesoporous carbon at low temperature since Zn^{2+} may act as chemical activator while silica and boric acid as pore templates to create large mesopore. Previously, ZBS was used as activator to prepare mesoporous carbon from fructose at low temperature (450°C). It resulted in the mesoporous carbon with pore size uniformity centered at ~ 30 nm [18]. However, it was not clear what component in ZBS that controls the

pore formation. The other researcher reported that ZBS ceramics contains zinc borate and zinc silicate crystals [19]. Information about the pore size controlling component of ZBS will have further chance of research, especially about substitution of the component which not controls the pore size with others.

In this study, mesoporous carbon was synthesized using activators of ZB, ZS, and ZBS. Correlation between the role of ZB and ZS in ZBS as pore controllers and their properties, including crystalinity, caramelization catalyst, and pyrolisis activator will be investigated.

2. Experimental:

2.1. Synthesis of mesoporous carbon: This research procedure is refered to our previous research [18], but with more amount of silica. All chemicals, including D-fructose, $ZnCl_2$, HCl (37%), H_3BO_3, HF (48%), were purchased from Merck and used as received without further purification process. A 10 g of fructose, 20 g of silicagel, 10 g of $ZnCl_2$, 12.35 g of H_3BO_3, and 60 mL of the distilled water was stirred in the beaker glass. The mixture was then heated at 100^oC for 4h under stirring. The obtained brown solid was heated at 130^oC for 1 h to form composite of caramel – activator in the oven. The composite was carbonized at 450^oC for 2 h under nitrogen gas flow to form composite of carbon – activator. The composite of carbon – activator was washed with 48% HF solution, 1M HCl solution, and distilled water respectively to separate the activators from the carbon. Then, the carbon product (carbon – ZBS) was dried at 130^oC for 6 h. The mesoporous carbons were sieved to get sizes of 100 – 120 mesh and characterized. Similar procedure was adopted without one of ZBS ceramics' precursor, including procedure without silica gel and boric acid. The resulted carbon powder was denoted as carbon -ZB, and carbon-ZS, respectively. Only carbon – ZB was washed without HF solution. As comparison, the powder activators were prepared using similar procedures without fructose.

2.1. Characterizations: The functional groups of carbon were determined by FTIR spectrophotometer (Shimadzu) using KBr pellet method. Adsorption-desorption nitrogen

isotherms were measured at–196^oC by Surface Area Analyzer (Quantachrome NovaWin2) after degassing the carbons at 130^oC for 3 h. Mesopore volume and pore size distribution were obtained from each adsorption and desorption plots by a Pierce Orr Dalla Valle (POD) analysis (Lowell et al , 2004). Crystal structures were evaluated using X-ray diffractometer (Philip) with Cu-Kα radiation ($\lambda = 1.5418$ Å), 2θ range between 5° and 90° and the scan step size of 0.017°. The morphology of the carbon was characterized using Transmission Electron Microscope (JEOL/EO). Absorbance of caramel intermediate (5 – hydroxymethyl furfural) was measured with UV-Vis spectrophotometer (Shimadzu).

3. Results and Discussions:

The N_2 adsorption desorption isotherm of the resulted carbon powders are presented in Figure (1). It is shown that carbon-ZB, carbon-ZS, and carbon-ZBS have similar isotherm curve patterns of type IV isotherms with hysteresis loop, characteristics of mesoporous material [20].
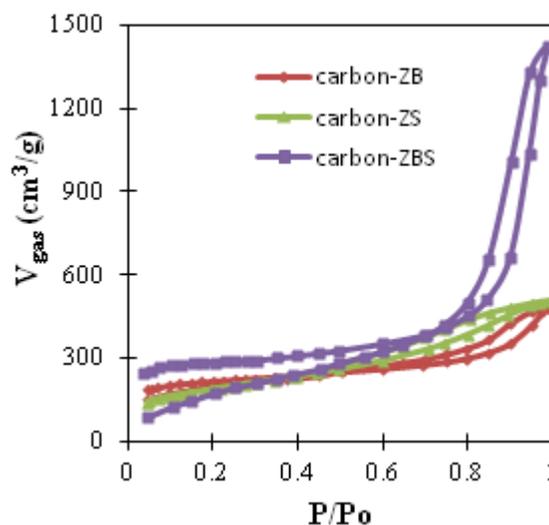

Figure (1): Adsorption – desorption isotherm curves of the mesoporous carbons synthesized with ZS, ZB, and ZBS activators

Both carbon – ZB and carbon – ZBS has the inflection points at P/Po ≈ 0.9 (adsorption) dan P/Po ≈ 0.85 (desorption). Those inflection points indicate pore uniformity. However, the curve inflection of carbon – ZBS is much longer and sharper than of carbon-ZB, indicating the higher uniformity. This prediction is confirmed further in Figure (3).

2

Mesopore volume distribution is shown in Figure (2). Value of mesopore volume was calculated based on adsorption and desorption isotherm data, as previous research [14]. The value was determined in 2 different pore size ranges to investigate difference of performance between ZB and ZS in forming large mesopore (> 100 Å).
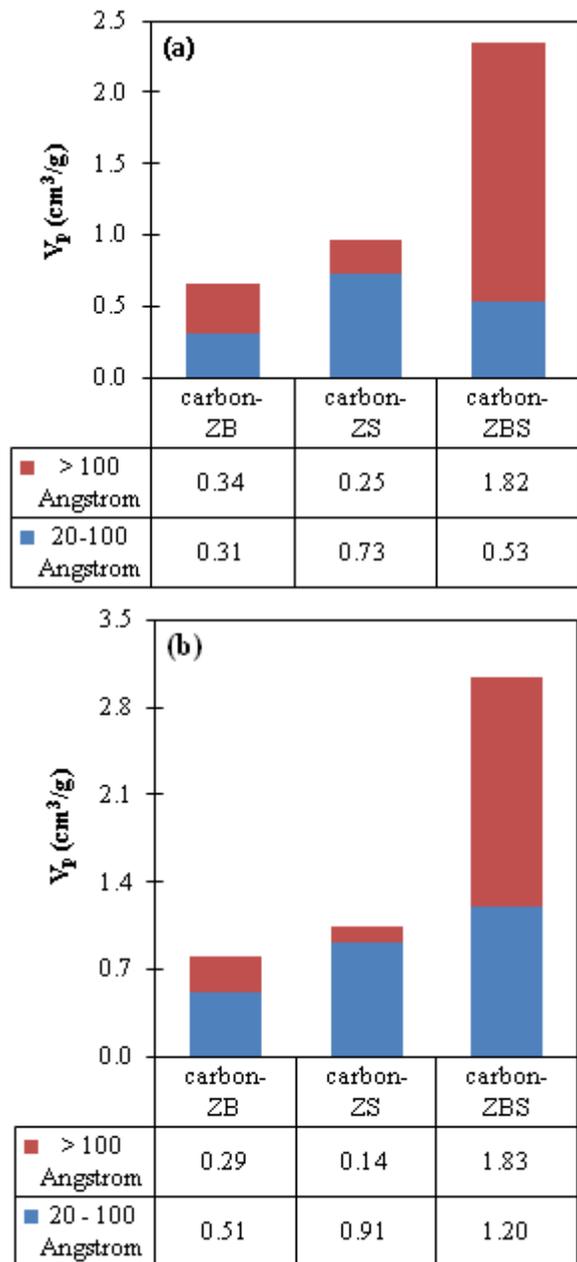

Figure (2): Mesopore volume distribution of the mesoporous carbons synthesized with various activators based on: a) adsorption data, b) desorption data

Figure (2) shows that ZB creates higher V_{meso} in the pore size range > 100 Å than ZS. However,

ZBS has much more mesopore volume in the same Å than ZB. It means that addition of silica into ZBS system improves formation of large mesopore zone. These patterns of pore volume distributiosn are influenced by patterns of pore size distributions in Figure (3).

In Figure (3), it is shown that both carbon-ZBS and carbon-ZB have pore uniformity at same places, including at 300 Å (based on adsorption data) and 180 Å (based on desorption data). However, peak of the carbon – ZBS is higher than the carbon – ZB. It indicates that ZB component in ZBS has the role to control mesopore size, whereas silica component in ZBS has the role to improve mesopore volume without changing the pore size. In other side, carbon-ZS has uniformity at low mesopore size (20 – 100 Å).
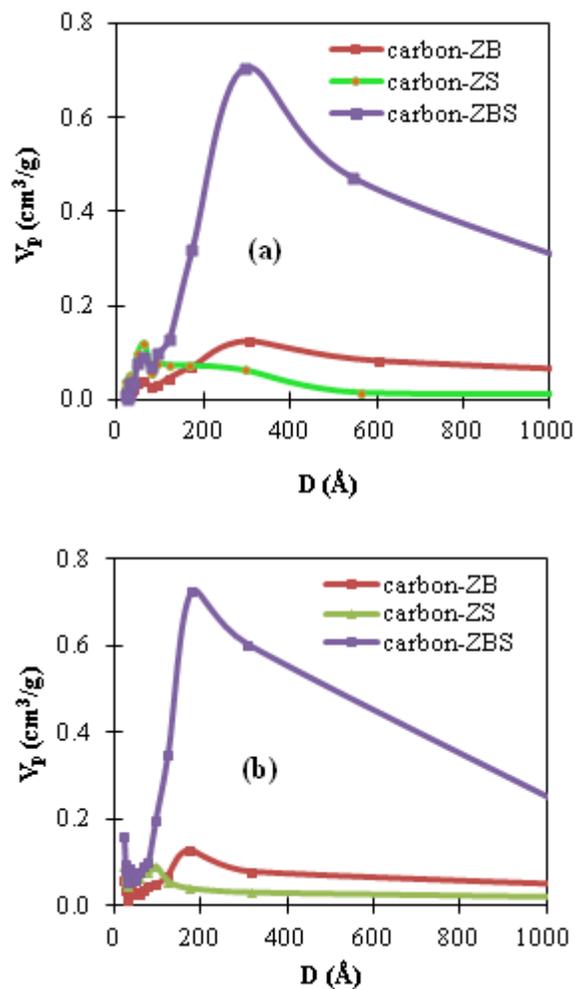

Figure (3): Pore size distribution of mesoporous carbon from fructose with various activator based on : a) adsorption data, b) desorption data
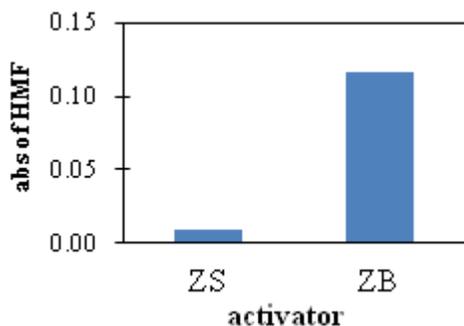
Figure (4): HMF absorbance of fructose solution 100 g/L after caramelization at 100^oC for 1 h with catalyst of ZS (zinc silicate) and ZB (zinc borate).

To understand why ZB can control mesopore size but ZS can not, role of activator as catalyst of caramelization, pore template, and pyrolisis activator were investigated. The role as catalyst of caramelization is detected from production of 5 – hydroxymethylfurfural (HMF). HMF is intermediate of caramel in caramelization reaction. The HMF has been used to detect caramel in sugar solution [21, 22]. Absorbance of HMF is measured with UV-Vis spectrophotometry (Figure 4).

Figure (5) shows that ZB gives much higher absorbance of HMF than ZS. It indicates that ZB supports much higher amount of the caramel product in the caramelization process than ZS. More amount of HMF gives more amount of caramel, precursor of pore wall.

To understand role of activators in carbonization reaction, characterization of the carbon was conducted with FTIR spectrophotometry. The FTIR spectra of the carbons is reported in Figure (5). Generally, Figure (5) exhibits peaks in 1207.36 cm^{-1}, 1586.34 cm^{-1}, 1698.21 cm^{-1}, and 3422.45 cm^{-1}. Those peaks of FTIR spectra characterize C-O, C=C at aromatics rings, C=O, and O-H bonds, respectively [23, 24, 25]. The OH bond can be attributed to the surface hydroxyl groups or the adsorbed H_2O. The C=O bond may be ketone, lactone, or carboxyl [24].

Figure (5) showed that carbon-ZS has the weaker bands than carbon-ZB. It indicates that ZS is stronger dehydrating agent than ZB. At 450^oC, surface of silica still contains germinal and

isolated silanol [26]. Those functional groups may act as dehydrating agent in carbonization process. However, no correlation between level of chemical activator strength in pyrolisis with mesoporosity of the carbon.
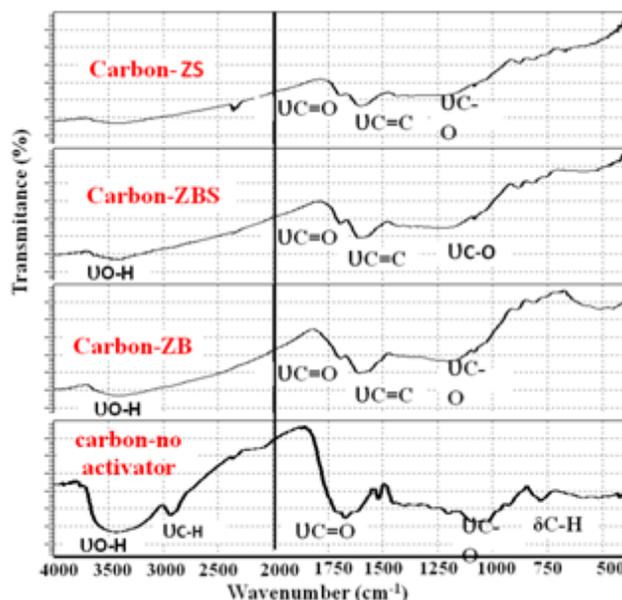

Figure (5): FTIR spectra of the mesoporous carbon from fructose with various activators.

To understand role of activator as pore template, characterization of activators with X-ray diffraction was conducted. The X-ray diffractograms of the activators are reported in Figure (6).

In Figure (6), ZBS ceramics exhibits some peaks of diffractograms. Based on standard diffractograms of ICDD 2013 no. 01-070-1235, ICDD 2013 no.00-027-1487, and PDF no. 321465, ZBS contains crystals of ZS (Zn_2SiO_4), ZB ($Zn_3B_2O_6$), and ZBH ($Zn_6B_{10}O_{21}.3H_2O$). Individually, ZB shows a high peak of diffractogram, whereas ZS shows wide peak, indicating the crystal structure and amorph, respectively. It indicates that formation of ZB crystal is easier than ZS in condition of this research. Based on atom radii data [27], bond distance of B-O is smaller than Si-O so that effect of breaking the bond by Zn^{2+} toward the B-O bond is lower than the Si-O. In other side, based on electroneganivity data [28], polarity of B-O is lower than Si-O so that effect of solvation toward the B-O bond is weaker than the Si-O.

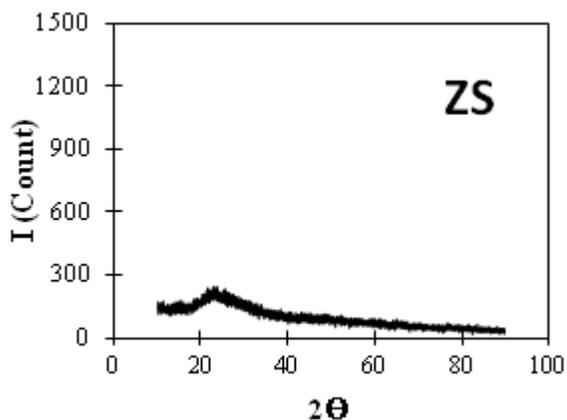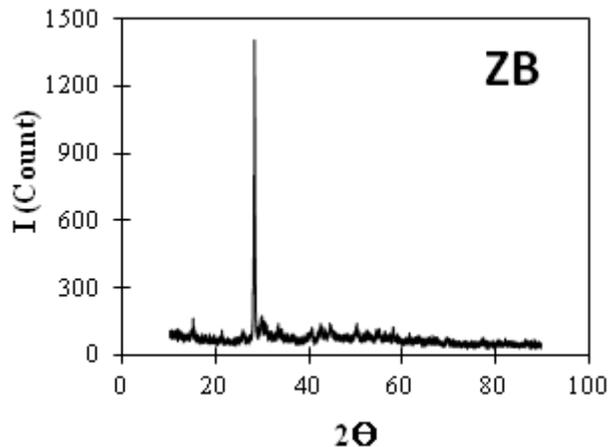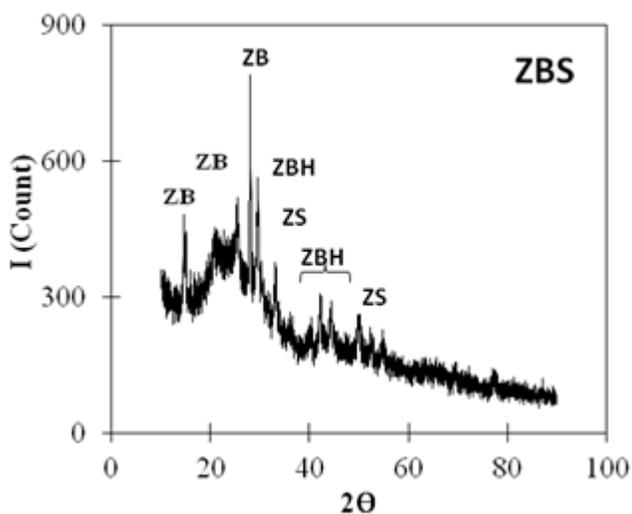This solvation may disturb formation of framework.

Figure (6): Diffractograms of ZBS, ZB, and ZS synthesized at calcination temperature of 450°C

Some peaks of ZB and ZBH in diffractogram of ZBS indicate that silica component in ZBS system improves crystalinity of ZB and ZBH. Negative charge of silicate may repell negative charge of borate ions which make borates easier both to make bond with Zn^{2+} cations and to form larger zinc borate framework than without the silicate addition. Chemical structures of zinc borate and zinc silicate with negative charges are designed in Figure (7).
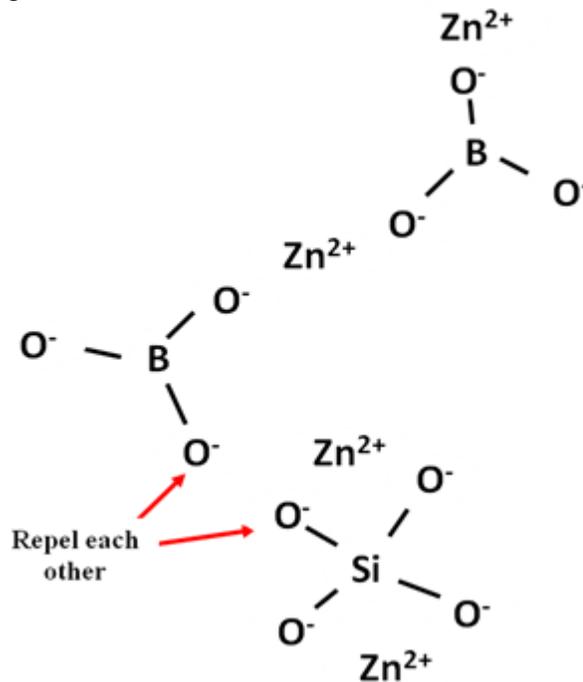

Figure (7): Chemical structure of ZS and ZB

Characterization of the carbons with X-ray diffraction method was conducted to investigate influence of activator formation toward crystal structure of the mesoporous carbon. The diffractograms are presented in Figure (8).

The diffractograms in Figure (8) show that all carbons have the wide peaks of diffractograms. It means that contain amorph structure. All carbon have main peak at about 21° (d = 4 Å). These peaks are far enough from main peak of standard graphite (2 thetha = 26.5^{o}) which indicate low quality of graphite. The d value > 3,34 Å indicates turbostratics structure [29]. Turbostratics is an intermediate structure between graphite and amorph [30].

The pore and pore wall morphology of the carbon-ZBS was characterized with TEM. Result of the characterization is reported in Figure (9).
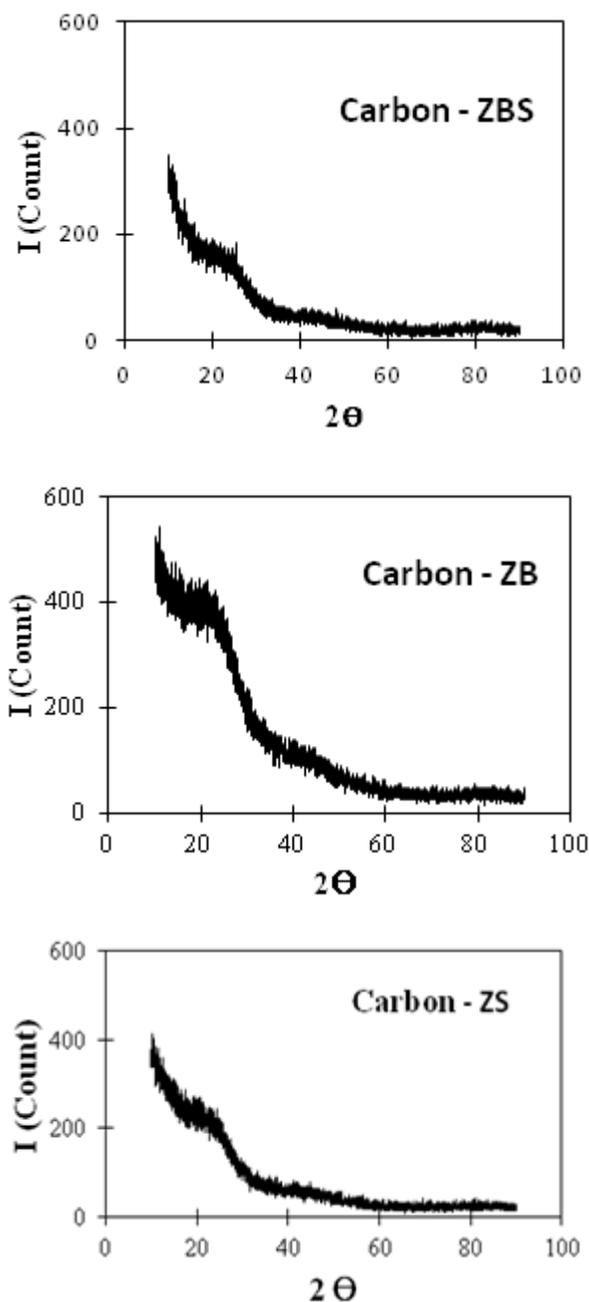
Figure (8): Diffractograms of the mesoporous carbon from fructose with various activator

Figure (9): Pore morphology pattern (a) and diffraction mode (b) of the carbon synthesized from fructose with ZBS activator at temperature of 450°C

4. Conclusions:

Mesoporous carbons have been synthesized from fructose with ZBS and components of ZBS activator, including zinc silicate and zinc borate,. Characterization toward physicochemistry of the carbons were performed, including pore, crystal structure, and functional group of the carnon surface. The investigation gives conclusion that zinc borate is the component of ZBS activator which controls pore uniformity of the carbon in 300 Å and 180 Å. Effectivity of ZB as caramelization catalyst and crystalinity of ZB may influence mesoporosityof the carbon. No correlation between chemical activation strength and crystalinity of ceramics with crystal structure of the carbon. All components of ZBS create the turbostratics structure of the carbon.

Figure (9) shows that the synthesized carbon has pores which are connected each other (white part). No pattern is exhibited by pore wall (black part). It indicates amorph structure. The diffraction mode in Figure (9b) shows pattern of rings and diffuse. It indicates mixture of amorph and polycrystaline [31].
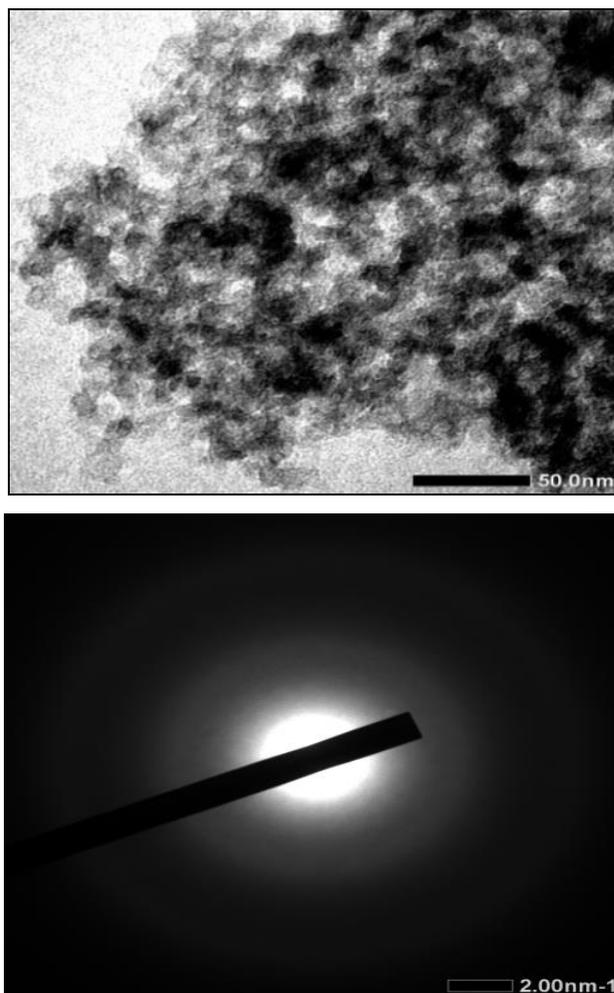
References :

1. E. Lorenc – Grabowska, G. Gryglewic, Dyes and Pigments 75 (2007)136

2. J. A. Fernandez, T. Morishita, M. Toyoda, M. Inagaki, F. Stoeckli, T. A. Centeno, J. Power Sources 175 (2008) 675.

3. Z. Xia, L. Liao, S. Zhao, Materials Research Bulletin 44 (2009) 1626.

4. M. Ulfa, W. Trisunaryanti, I. I. Falah, I. Kartini, Sutarno, IOSR Journal of Applied Chemistry 7/5 (2014) 01.

5. S. Han, Y. Yun, K. W. Park, Y. E. Sung, T. Hyeon, Adv.Mater. 15/22 (2003) 1922.

6. S. Geranmayeh, A. Abbasi, A. Badiei, E-Journal of Chemistry 8/1 (2011) 196.

7. G. W. Markus, P. Peduzzi, Mar. Ecol. Prog. Ser. 108 (1994) 11.

8. L. Ying, L. Z. Jian, Y. Z. Xia, L. G. Jun, T. H. Dong, I. U. H. Zhang, New Carbon Materials 26/2(2011).

9. W. Dai, M. Zheng, Y. Zhao, S. Liao, G. Ji, J. Cao, Nanoscale Res. Lett. 5/1 (2010) 103.

10. N. Wickramaratne and M. Jaroniec, RSC Adv. 2(2012) 1877.

11. K. Chen, L. Kang, M. Zhu, and B. Dai, Catal. Sci. Technol. 5 (2015) 1035.

12. H. Lee, J. H. Kim, D. J. You, J. E. Lee, J. M. Kim, W. M. Ahn, C. Pak, S. H. Joo, H. Chang, and D. Seung, Adv. Mater. 20 (2008) 757.

13. H. I. Lee, G. D. Stucky, J. H. Kim, C. Pak H. Chang, J. M. Kim, Adv. Mater. 23 (2011) 2357.

14. Y. Onal, A. C. Basar, C. Sanci-Ozdemir, and S. Erdogan, J. Hazard Mater. (2006) 1698.

15. J. Hayashi, A. Kazehaya, K. Muroyama, A. P. Watkinson, Carbon 38 (2000) 1873.

16. Z. Zhu, A. M. Li, M. Xia, J. Wan and Q. Zhang, Chinese Journal of Polymer Science 26/5 (2008) 645.

17. Y. Huang, S. Hu, S. Zuo, Z. Xu, C. Han, J. Shen, J. Material Chemistry 19 (2009) 7759.

18. T. Setianingsih, I. Kartini, Y. Arryanto, Indo. J. Chem. 14/3 (2014) 253.

19. S. O. Yoon, K. S. Jo, Kim, S. Kim, Ceramics International 34(2008) 2155.

20. S. Lowel, J. E. Shield, M. A. Thomas, M. Thommes, Characterization of Porous Solids and Powders: Surface Area, Pore Size, and Density, Kluwer Academic Publishers (2004) 38 – 40.

21. B. F. M. Kuster, Eindhoven, Starch 42/8(1990) 314.

22. M. Boscolo, G. Luiz, A. Sobrinho, S. Benedito, L. Neto, D. W. Franco, J. AOAC Int. 85/3 (2002).

23. S. P. Chayande, Singha, and M. K. N. Yenkie, Chem Sci Trans. 2/3 (2013) 835.

24. A. M. Puziya, O. I. Poddubnayaa, A. Mart´ınez-Alonsob, F. Sua´rez-Garc´ıab, J. M. D. Tasco, Carbon 40 (2002) 1493.

25. A. C. Lua, T. Yang, Journal of Colloid and Interface Science 290 (2005) 505.

26. L. T. Zhuravlev, Physicochem. Eng. Aspects 173 (2000) 1.

27. S. M. Owen, A. T. Brooker, A Guideto Modern Inorganic Chemistry, Longman Singapore Publisher Pvt. Ltd. (1994) 58 and 65.

28. D. F. Shriver, P. W. Atkins, C. H. Langford Inorganic Chemistry, Oxford Univrsity Press (1990) 31.

29. L. Zou, Y. Huang, Q. Huang, C. Wang, Mater. Chem. Phys. 82 (2003) 654.

30. B. Manoj, A. G. Kunjomana, Int. J. Electrochem. Sci. 7 (2012) 3127.

31. Y. Leng, Materials Characterization: Introduction to Microscopic and Spectroscopic Methods, John Wiley & Sons (Asia) Pvt. Ltd. (2008) 108.